

## Comparative study of the equatorial ionosphere over Jicamarca during recent two solar minima

Libo Liu,<sup>1,2</sup> Jun Yang,<sup>1,3</sup> Huijun Le,<sup>1</sup> Yiding Chen,<sup>1</sup> Weixing Wan,<sup>1</sup> and Chien-Chih Lee<sup>4</sup>

Received 30 September 2011; revised 22 November 2011; accepted 22 November 2011; published 21 January 2012.

[1] It is a critical issue that whether or not the extremely deep solar minimum of solar cycle 23/24 brought serious influences on the Earth's space environment. In this study, we collected and manually scaled the ionograms recorded by a DPS ionosonde at Jicamarca (12.0°S, 283.2°E) to retrieve  $F$  layer parameters and electron density ( $N_e$ ) profiles.

A comparative study is performed to evaluate the equatorial ionosphere in solar minima of cycle 22/23 (1996–1997) and 23/24 (2008–2009). The seasonal median values of the critical frequency of  $F_2$  layer ( $f_oF_2$ ) were remarkably reduced in four seasons during the deep solar minimum, compared to those in 1996–1997. It is the first time to find that lower values prevail at most times in 2008–2009 in the  $F_2$  layer peak height ( $h_mF_2$ ) and Chapman scale height ( $H_m$ ). The bottomside profile thickness (B0) shows higher values in 2008–2009 than that in 1996–1997 at some daytime intervals, although it also becomes smaller during the rest times. Furthermore, the ionosphere in 2008–2009 is contracted strongly at altitudes above  $h_mF_2$  and more perceptible in the afternoon hours. The decrease in  $N_e$  is strongest in September equinox and weakest in June solstice. The ionospheric responses from solar minimum to minimum are mainly caused by the reduction in solar extreme ultraviolet intensity, and the contribution from dynamical processes competes and is variable. Analysis reveals that semiannual and longer-scale components are certainly reduced during the deep solar minimum, while shorter scale (e.g., 4 month) components may disrupt the decline picture at some times.

**Citation:** Liu, L., J. Yang, H. Le, Y. Chen, W. Wan, and C.-C. Lee (2012), Comparative study of the equatorial ionosphere over Jicamarca during recent two solar minima, *J. Geophys. Res.*, 117, A01315, doi:10.1029/2011JA017215.

### 1. Introduction

[2] Among recent several solar cycles, the solar activity during the minimum of solar cycle 23/24 was record low and unusually long lasting. The deep solar minimum for the years 2008–2009 has become an important issue in various fields of space physics, especially in the ionosphere and upper atmosphere physics [e.g., Araujo-Pradere et al., 2011; Chen et al., 2011; Emmert et al., 2010; Gibson et al., 2009; Heelis et al., 2009; Liu et al., 2009, 2011a; Lühr and Xiong, 2010; Russell et al., 2010; Solomon et al., 2010]. Gibson et al. [2009] and Russell et al. [2010] characterized significant variations in the solar-heliospheric-geospace system during this deep solar minimum. There is  $\sim 15\%$  reduction in solar extreme ultraviolet (EUV) radiance from solar cycle 22/23 minimum (1996–1997) to recent minimum (2008–2009) [Didkovsky et al., 2010; Solomon et al., 2010]. The upper atmosphere became unprecedentedly cooler and thinner in

2008–2009, causing a decrease in the thermospheric mass density by about 30% at 400 km altitude [Emmert et al., 2010]. Simulation results support the reduction in solar EUV intensity being the primary contributor to the thermosphere cooling during the deep minimum period [Solomon et al., 2010, 2011].

[3] Liu et al. [2011a] collected the ionosonde data at worldwide stations provided from the Solar Physics Interactive Data Resource (SPIDR) website (available at <http://spidr.ngdc.noaa.gov/>) to examine the changes in the ionospheric electron density ( $N_e$ ) during this extreme solar minimum. Their analysis showed that in the recent solar minimum the daytime  $F_2$  layer critical frequency ( $f_oF_2$ ) or peak electron density ( $N_mF_2$ ) dropped to the recorded lowest levels.  $f_oF_2$  (in MHz) is related to  $N_mF_2$  (in electrons/m<sup>3</sup>) by the equation  $N_mF_2 = 1.24 \times 10^{10} \times (f_oF_2)^2$ . Remarkable reduction was simultaneously detected in the global-average total electron content (TEC) in the ionosphere, which were obtained from the Global Ionospheric Maps (GIMs) produced by Jet Propulsion Laboratory (JPL).

[4] Discernible changes were also detected in the topside ionosphere. Ionospheric empirical models overestimate the observed upper transition height, ion temperature and electron density ( $N_e$ ) in the topside ionosphere in 2008 [Heelis et al., 2009; Lühr and Xiong, 2010]. In contrast, the models provide reasonable predictions of these parameters observed during other periods. Therefore, during the deep

<sup>1</sup>Beijing National Observatory of Space Environment, Institute of Geology and Geophysics, Chinese Academy of Sciences, Beijing, China.

<sup>2</sup>Also at State Key Laboratory of Space Weather, Center for Space Science and Applied Research, Chinese Academy of Sciences, Beijing, China.

<sup>3</sup>Graduate University of Chinese Academy of Sciences, Beijing, China.

<sup>4</sup>General Education Center, Ching-Yun University, Jongli, Taiwan.

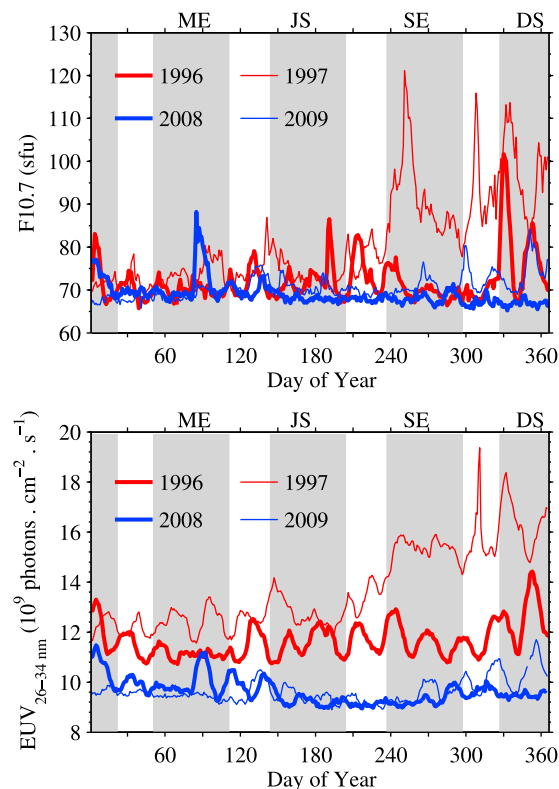


**Figure 1.** (top) Solar 10.7 cm radio flux index  $F_{10.7}$  and (bottom) solar full-disk 26–34 nm EUV flux during the last solar minimum (1996–1997) and the recent solar minimum (2008–2009).  $F_{10.7}$  is adjusted to 1 AU, in solar flux units (sfu,  $1 \text{ sfu} = 10^{-22} \text{ W m}^{-2} \text{ Hz}^{-1}$ ). The daily average intensity of EUV flux in unit of  $10^9 \text{ photons cm}^{-2} \text{ s}^{-1}$  is recorded by SOHO/SEM. Shaded areas indicate the intervals of four seasons, March Equinox (ME), June Solstice (JS), September Equinox (SE), and December Solstice (DS), in the analysis.

solar minimum the ionosphere may exhibit characteristics substantially different from the previous solar minima [Lühr and Xiong, 2010]. Recently, [Araujo-Pradere et al., 2011] also detected a decrease in TEC over local regions, but it is interesting that they found a minor and marginal in  $N_m F_2$  at four middle latitude stations. It is notable that the analysis of Araujo-Pradere et al. [2011] was made by directly comparing with monthly average data in selected months.

[5] Therefore, different studies reported inconsistent changes in  $N_m F_2$  from solar minimum to minimum. The conflicting results certainly call for further investigation to gain a better understanding of the ionospheric behavior under such unusual solar conditions, to examine the data consistency, and to determine the influence of analysis techniques applied. Moreover, up to now, there are few investigations on changes in the  $F$  layer parameters and  $N_e$  profiles in the equatorial ionosphere, especial the  $F_2$  layer peak height  $h_m F_2$ , during the current unusual solar minimum.

[6] In the current analysis, we retrieved  $N_e$  profiles from measurements by a DPS Digisonde at Jicamarca ( $12.0^\circ\text{S}$ ,  $283.2^\circ\text{E}$ ; dip  $0.28^\circ$ ) in 1996–1997 and 2008–2009 to elucidate possible changes in equatorial ionosphere during the last two solar minima. Our focus is on the changes in ionogram-derived  $N_e$  profiles and  $F$  layer parameters from

solar minimum to minimum. The  $F$  layer parameters consist of  $N_m F_2$ ,  $h_m F_2$ , Chapman scale height  $H_m$ , and the bottom-side thickness parameter  $B0$ . It is the first time to report the response of equatorial ionosphere to the anomalous decrease in solar EUV input. Our analysis identifies a reduction in  $N_m F_2$  over Jicamarca during both the daytime and nighttime. The reduction in the Chapman scale height  $H_m$ ,  $h_m F_2$ , and the bottomside thickness parameter  $B0$  is prevailing over most times, but in certain instances marginal or minor responses are also detected in  $h_m F_2$ ,  $H_m$  and  $B0$ . An outstanding feature is higher  $B0$  in 2008–2009 than in 1996–1997 at some daytime intervals.

## 2. Data Source

[7] Figure 1 (top) illustrates the evolution of solar 10.7 cm radio flux index  $F_{10.7}$  for 4 years (1996, 1997, 2008, and 2009), and Figure 1 (bottom) plots the daily values of solar full-disk EUV intensity at 26–34 nm wavelengths, which were monitored by Solar and Heliospheric Observatory/Solar EUV Monitor (SOHO/SEM) [Judge et al., 1998]. The SOHO/SEM EUV data were distributed by the Space Sciences Center of University of Southern California. Both  $F_{10.7}$  and the SOHO/SEM EUV used here are values normalized to 1 AU. In this analysis, the data within  $\pm 30$  days around the March equinox (ME), June solstice (JS), September equinox (SE) and December solstice (DS) are designated as the four seasons and labeled as ME, JS, SE and DS for brevity at the top of the panels in Figure 1, respectively. The shaded areas superimposed in Figure 1 indicate the day of year (DoY) intervals for the four seasons.

[8] To gauge what changes occurred in the recent solar minimum, we divide the data into two groups for a comparative study; one includes the data for the years 1996–1997 and the other includes the data for the years 2008–2009. By comparing the two groups, we could determine the solar minimum-to-minimum differences of the parameters and electron density profiles. The seasonal mean values of  $F_{10.7}$  and SOHO/SEM EUV in four seasons corresponding to the two groups are given in Table 1.

[9] As indicated by the values of  $F_{10.7}$  in Figure 1 and the 120 day seasonal mean values in Table 1, the solar activity was generally low (seasonal mean  $F_{10.7}$  are  $\sim 70$  sfu;  $1 \text{ sfu} = 10^{-22} \text{ W} \cdot \text{m}^{-2} \cdot \text{Hz}^{-1}$ ) in 1996–1997 and 2008–2009. An exception is that seasonal mean  $F_{10.7}$  have higher values ( $\sim 80$  sfu) in the second half year of 1997. In addition,

**Table 1.** Mean Values of  $F_{10.7}$  and EUV in Four Seasons During the Last Two Solar Minima<sup>a</sup>

	March Equinox	June Solstice	September Equinox	December Solstice
$F_{10.7}$ in 1996–1997	71.98	72.80	80.77	82.52
$F_{10.7}$ in 2008–2009	70.24	69.35	69.34	70.30
$\Delta F_{10.7}$	1.74	3.45	11.43	12.22
EUV in 1996–1997	11.79	12.13	13.51	13.69
EUV in 2008–2009	9.69	9.35	9.43	10.02
$\Delta \text{EUV}$	2.10	2.78	4.08	3.67

<sup>a</sup>Here  $F_{10.7}$  is the seasonal mean value of daily 10.7 cm flux in solar flux units ( $1 \text{ sfu} = 10^{-22} \text{ W m}^{-2} \text{ Hz}^{-1}$ ) and EUV (in  $10^9 \text{ photons cm}^{-2} \text{ s}^{-1}$ ) is the seasonal mean value of SOHO/SEM EUV at 26–34 nm wavelengths.  $\Delta F_{10.7}$  and  $\Delta \text{EUV}$  are the corresponding seasonal difference of  $F_{10.7}$  and EUV in 1996–1997 from that in 2008–2009.

several spikes appeared infrequently in the other 3 years. Table 1 also shows the differences of seasonal mean  $F_{10.7}$  between the two periods, varying from 1.7 sfu in March equinox to 12.2 sfu in December solstice. As seen from Figure 1, the intensity of SOHO/SEM EUV was around  $9.3 \sim 10.0 \times 10^9$  photons  $\text{cm}^{-2} \text{s}^{-1}$  in 2008 and 2009 and  $11.8 \sim 13.7 \times 10^9$  photons  $\text{cm}^{-2} \text{s}^{-1}$  in 1996 and 1997. Therefore, as pointed out by *Chen et al.* [2011],  $F_{10.7}$  fails to reliably indicate the intensity of SOHO/SEM EUV in 2008–2009. According to Table 1, the seasonal mean values of SOHO/SEM EUV differed by about  $2.1 \sim 4.1 \times 10^9$  photons  $\text{cm}^{-2} \text{s}^{-1}$  between the last two solar minima, showing larger differences than  $F_{10.7}$ . Another interesting feature is that the SOHO/SEM EUV intensity showed significant solar rotation signatures in 1996–1997, but this signature disappeared or became very weak at most times in 2008–2009. Furthermore, the pressure, flux, and magnetic flux of solar wind during 2008–2009 were observed at their lowest levels; as a result, the geomagnetic activity also became quieter during the recent solar minimum [*Chen et al.*, 2011].

[10] In this study, we collected the ionograms recorded by a DPS ionosonde at Jicamarca during the last two solar minima, 2 years data (1996–1997) for the last minimum and 2 years (2008–2009) for the recent minimum. The ionogram records were downloaded from the Lowell Digital Ionogram DataBase (DIDBase) [*Reinisch et al.*, 2004a]. We have manually edited the 4 year ionogram traces and used the SAO-Explorer software to retrieve  $N_e$  profiles by using the built-in true height inversion algorithm [*Huang and Reinisch*, 1996]. The SAO-Explorer software is an interactive ionogram scaling environment, which also has capability of accessing ionograms and ionogram-derived data from more than 60 locations in the Lowell DIDBase.

[11] We chose the ionogram-derived  $F$  layer parameters  $f_oF_2$ ,  $h_mF_2$ , B0 and  $H_m$  at Jicamarca for this analysis. Here B0 is the thickness parameter, measuring the thickness of the bottomside  $F_2$  layer profile [*Gulyaeva*, 1987]. When B0 is introduced, the electron density profile  $N_e(h)$  in the bottomside ionosphere can be represented as

$$N_e(h) = \frac{N_m F_2 \exp(-x^{B_1})}{\cosh(x)}, \quad x = \frac{h_m F_2 - h}{B_0}. \quad (1)$$

The shape parameter  $B_1$  in equation (1) determines the shape of the profile between  $h_m F_2$  and  $h_{0.238}$  (the height where the value of  $N_e$  drops to  $0.238 N_m F_2$ ). See *Bilitza et al.* [2000] and *Gulyaeva* [1987] for the details. The Chapman scale height  $H_m$ , measuring the topside  $N_e$  profile slope [*Kutiev et al.*, 2009; *Liu et al.*, 2007], is determined by the  $N_e$  profile at altitudes around  $h_m F_2$  when the Chapman- $\alpha$  profile function

$$N_e(h) = N_m F_2 \exp\left\{\frac{1}{2} [1 - z - \exp(-z)]\right\}, \quad z = (h - h_m F_2)/H(h), \quad (2)$$

is adopted to analytically model the ionospheric profile [e.g., *Huang and Reinisch*, 2001].  $H_m$  is the value of scale height  $H(h)$  at  $h_m F_2$ . *Huang and Reinisch* [2001] developed a technique to approximately extrapolate the topside  $N_e(h)$  with equation (2) based on ionogram measurements. *Liu et al.* [2006] have investigated the seasonal variations of the ionogram-derived  $H_m$  over Wuhan (114.4°E, 30.6°N; dip

45.2°). They revealed that B0 is perfectly correlated with  $H_m$ . *Lee and Reinisch* [2007] also reported higher  $H_m$  in the winter months over Jicamarca in solar minimum.

[12] In the context of data analysis, some clarification is needed concerning the topside scale height derived by extrapolation of the bottomside electron density profile. *Reinisch et al.* [2004b] compared the topside profiles constructed with ionogram-derived Chapman scale height and observations from satellites and incoherent scatter radars in middle latitude and equatorial regions. Good agreement is found in their comparisons. However, *Tulasi Ram et al.* [2009] recently questioned the confidence in the topside profile based on simultaneous topside measurements from both satellite and the Jicamarca incoherent scatter radar. Therefore, the whole profile comparisons can provide us valuable information on the topside part, but it should be with caution that the confidence may become poorer at higher altitudes.

### 3. Results

#### 3.1. The $f_oF_2$ During the Last Two Solar Minima

[13] Figure 2 shows the universal time (UT) variation of Jicamarca  $f_oF_2$  in four seasons for the two solar minima. The blue line in each panel of Figure 2 corresponds to  $f_oF_2$  in 2008–2009, the red line for those in 1996–1997, and the black line shows  $\Delta f_oF_2$ , the differences of  $f_oF_2$  between the two groups. Positive  $\Delta f_oF_2$  means higher  $f_oF_2$  in 1996–1997 and negative  $\Delta f_oF_2$  means higher values in 2008–2009. The error bars superimposed in each panel describe the upper and lower quartiles. The local midnight and noon at Jicamarca is indicated by the solid and open semicircle, respectively, around the horizontal axis. Figures 3–5 are plotted in the similar style of Figure 2, but for  $h_m F_2$ , B0, and  $H_m$ , respectively.

[14] The number of data points as a function of universal time is given at the top of each panel in Figures 2 and 3. When spread- $F$  appeared in nighttime ionograms, the  $F$  layer traces cannot be unambiguously scaled to retrieve  $F$  layer parameters and  $N_e$  profile. Moreover, either strong absorption or no observations also result in data unavailable in some cases. Therefore, the data points in each season vary from 120 points to below 50 points (dotted line in Figure 2). The cases where the number of data is less than 50 are considered as that there are not enough data to reliably evaluate the corresponding seasonal median and upper and lower quartiles. As a consequence, gaps are seen in the nighttime.

[15] At altitudes in the upper atmosphere above Jicamarca, the sunretime is around 05:00–05:30 Local Time (LT) (10:00–10:30 UT). After sunrise, a rapid increase in  $f_oF_2$  can be found from 06:00 LT (11:00 UT) to 09:00 LT (14:00 UT) for the two groups in all seasons. Then the  $f_oF_2$  increment stops, or turns to decrease for several hours, and starts to increase once again in the afternoon. Thus, the diurnal evolution of  $f_oF_2$  forms either a daytime flat peak or a noon trough sandwiched between the morning and afternoon peaks. After the afternoon peak,  $f_oF_2$  decays steadily in the nighttime and reaches its minimum before the sunrise. This feature is the well-known noon-bite phenomenon [e.g., *Raju and Rao*, 1975]. The diurnal and seasonal variations of  $f_oF_2$  over Jicamarca during solar minimum have been investigated by *Lee et al.* [2008]. Thus, we focus on the solar minimum-to-minimum differences of ionospheric parameters.

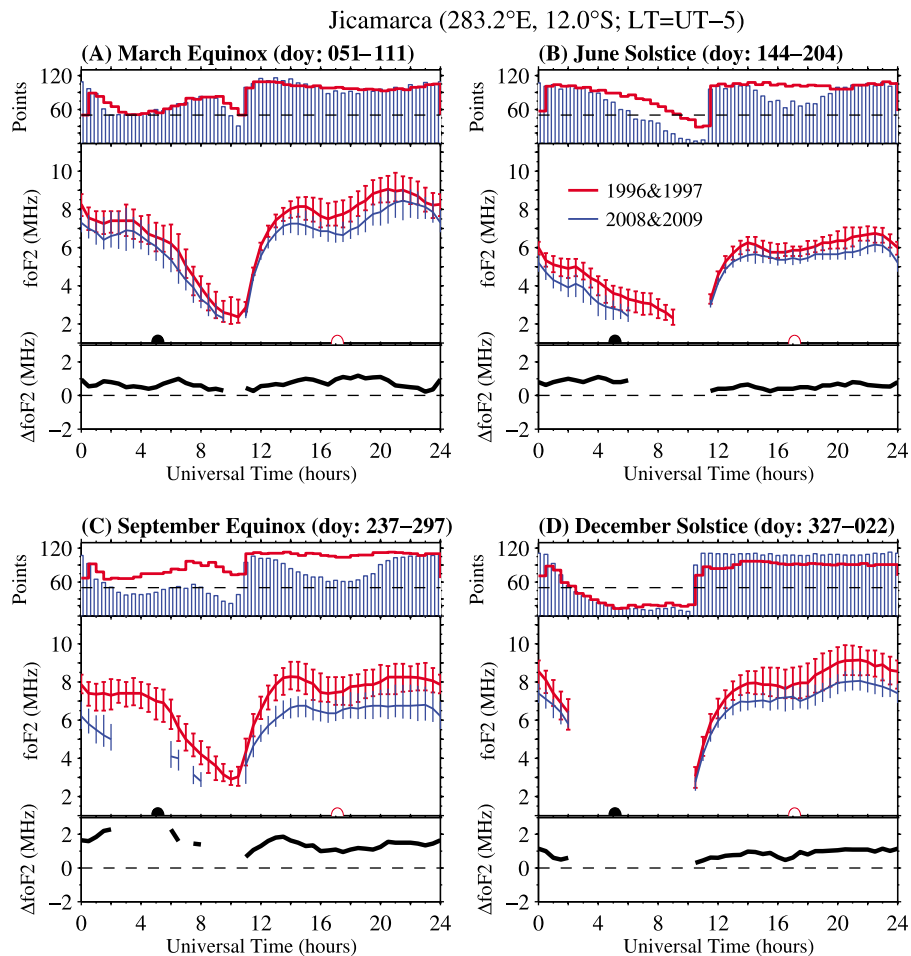


**Figure 2.** Universal time variation of  $f_oF_2$  ( $F_2$  layer critical frequency) over Jicamarca in four seasons for the last two solar minima. The red and blue lines indicate seasonal median  $f_oF_2$  in 1996–1997 and in 2008–2009, respectively, and  $\Delta f_oF_2$  is the differences. Bars show the corresponding upper and lower quartiles. The number of data points at universal times in each season is given at the top of each panel. The seasonal median and upper/lower quartiles are not calculated when the number of data is below 50 points (dotted line). The local midnight and noon at Jicamarca is indicated by the solid and open semicircle, respectively, on the horizontal axis.

[16] Seeing from Figure 2, we can find significant differences of  $f_oF_2$  between the two solar minima in all four seasons: the value of  $f_oF_2$  is overall smaller in 2008–2009 than in 1996–1997; smaller values of  $f_oF_2$  occurred not only in the daytime but also in the nighttime, although it is hard to safely quantify at the gaps. For the seasonal feature, one can see that the most notable differences between the two groups occurred in September equinox. The largest differences in September equinox are expected to be related to the difference in solar EUV radiation [Liu *et al.*, 2011a]. As shown in Table 1, the difference in EUV intensity from solar minimum to minimum is largest in September equinox.

### 3.2. The $h_mF_2$ , $H_m$ , and B0 During the Last Two Solar Minima

[17] Figure 3 shows the diurnal variations of Jicamarca  $h_mF_2$  in four seasons for the two solar minima. Generally, the seasonal median  $h_mF_2$  takes higher values in the daytime than in the nighttime. After sunrise,  $h_mF_2$  starts to rise rapidly from 07:00 LT (12:00 UT) to 10:00 LT (15:00 UT). Then  $h_mF_2$  stays at high levels, forming a peak around noon.

It descends slowly in the afternoon. Later,  $h_mF_2$  starts to rise and forms a sunset peak in all seasons, except in June solstice. Subsequently, the ionosphere declines gradually and reaches a midnight platform with low values. Moreover,  $h_mF_2$  at Jicamarca presents seasonal variations, showing differences in both the values and the diurnal variation pattern in four seasons. The most outstanding feature is that the sunset peak is best developed in the diurnal  $h_mF_2$  during March equinox but is absent during June solstice.

[18] Similar to  $f_oF_2$  as shown in Figure 2, the  $h_mF_2$  over Jicamarca in 2008–2009 is also overall lower than that in 1996–1997 for both daytime and nighttime. A slight difference is that there are only minor minimum-to-minimum differences in equatorial  $h_mF_2$  at 14:00–18:00 LT (19:00–23:00 UT) in December solstice. The  $h_mF_2$  difference is marginal around midnight in March equinox and at 01:00–03:00 LT (06:00–08:00 UT) in September equinox.

[19] Likewise, Figure 4 shows the diurnal variation of seasonal median  $H_m$  (the  $F_2$  layer Chapman scale height) at Jicamarca for the two solar minima in four seasons. We can see that the diurnal patterns of  $H_m$  are quite alike for the two

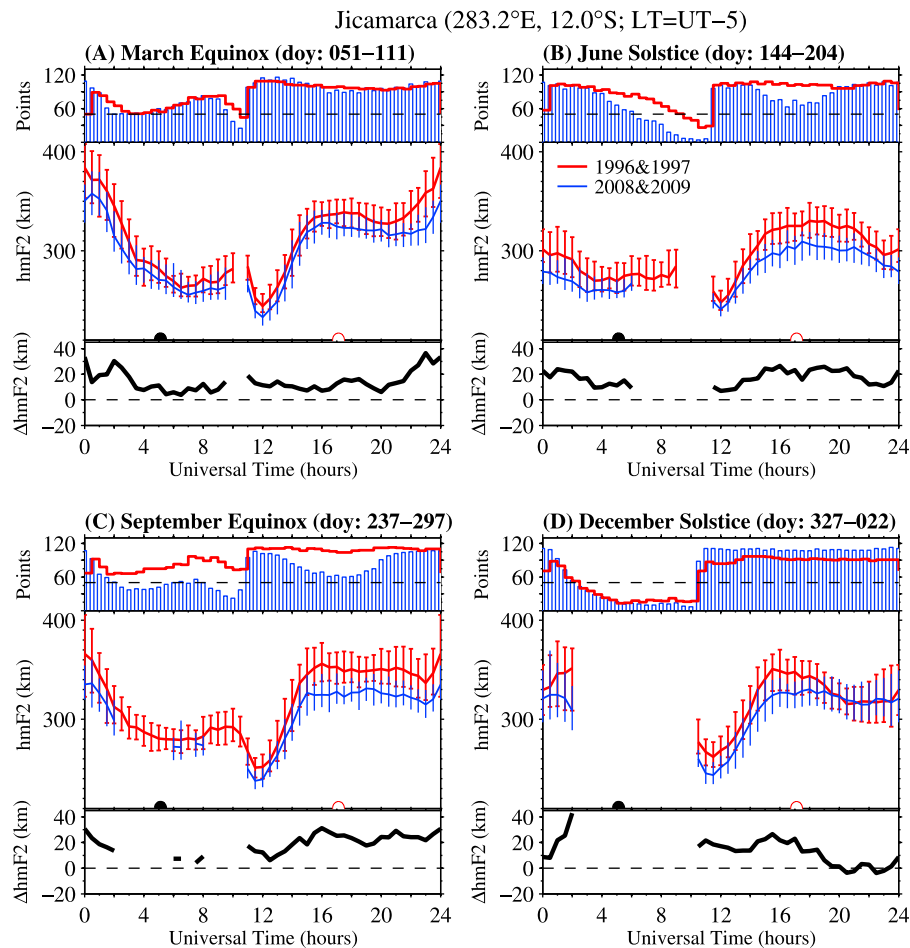


**Figure 3.** Similar to Figure 2, but for  $h_mF_2$  (the  $F_2$  layer peak height).  $\Delta h_mF_2$  is the difference of  $h_mF_2$  during the last two solar minima.

groups. A morning increase in  $H_m$  is followed by an afternoon decrease.  $H_m$  reaches its maximum around middaytime with values about 100 km or more and takes its minimum during the nighttime with values less than 50 km. There is no significant local time change in  $H_m$  during the nighttime compared with those in the daytime.

[20] As depicted in Figure 4, the values of  $H_m$  in 2008–2009 differ evidently from those in 1996–1997 all the time in June solstice. In contrast, in other three seasons they follow each other closely at some daytime intervals and differ from each other for the rest of the day. The  $H_m$  in 2008–2009 are lower than that in 1996–1997 for most times, but they are roughly identical at 10:00–16:00 LT (15:00–21:00 UT) in March equinox and during the morning hours in September solstice, and what's more is that the former exceeds the latter at 14:00–18:00 LT (19:00–23:00 UT) in December solstice. An outstanding feature in Figure 4 is that, although the values of  $H_m$  are larger in daytime, positive  $\Delta H_m$  prevails in nighttime.

[21] Figure 5 shows the universal time variation of B0 (the thickness parameter of the bottomside  $N_e$  profile) over Jicamarca for the two solar minima in four seasons. The diurnal variations of B0 are in the same style of those of  $H_m$ , which is well consistent with the finding of Liu *et al.* [2006] and Lee and Reinisch [2007]; that is, B0 is highly correlated with  $H_m$ .

[22] However, the minimum-to-minimum differences of B0 are more complicated than those of other parameters ( $f_oF_2$ ,  $h_mF_2$ , and  $H_m$ ).  $\Delta B0$  in Figure 5 shows that B0 in 2008–2009 is not consistently lower than in 1996–2007. Negative  $\Delta B0$  is found at some daytime interval of 09:00–15:00 LT (14:00–20:00 UT) in March equinox, June solstice and September equinox, and at 14:00–18:00 LT (19:00–23:00 UT) in December solstice.

### 3.3. $N_e$ Profiles

[23] It is true that the ionosonde can yield electron density profiles up to but not beyond the altitudes of  $h_mF_2$ . As mentioned in section 2, however, Huang and Reinisch [2001] have developed a technique to extrapolate the topside  $N_e(h)$ . The reliability of the extrapolated topside  $N_e(h)$  has been verified with incoherent scatter radar measurements over Jicamarca [Reinisch *et al.*, 2004b]. The comparisons indicated the SAO-Explorer retrieved electron density profiles are valuable for the ionosphere even up to several hundreds of kilometers above  $h_mF_2$ , but it should be noted that the confidence of the topside profile becomes poorer at higher altitudes. We get the electron density profiles up to the topside ionosphere altitudes over Jicamarca by scaling the ionograms with the SAO-Explorer.

[24] Figure 6 illustrates the universal time and altitude distributions of seasonal average  $N_e$  over Jicamarca in four

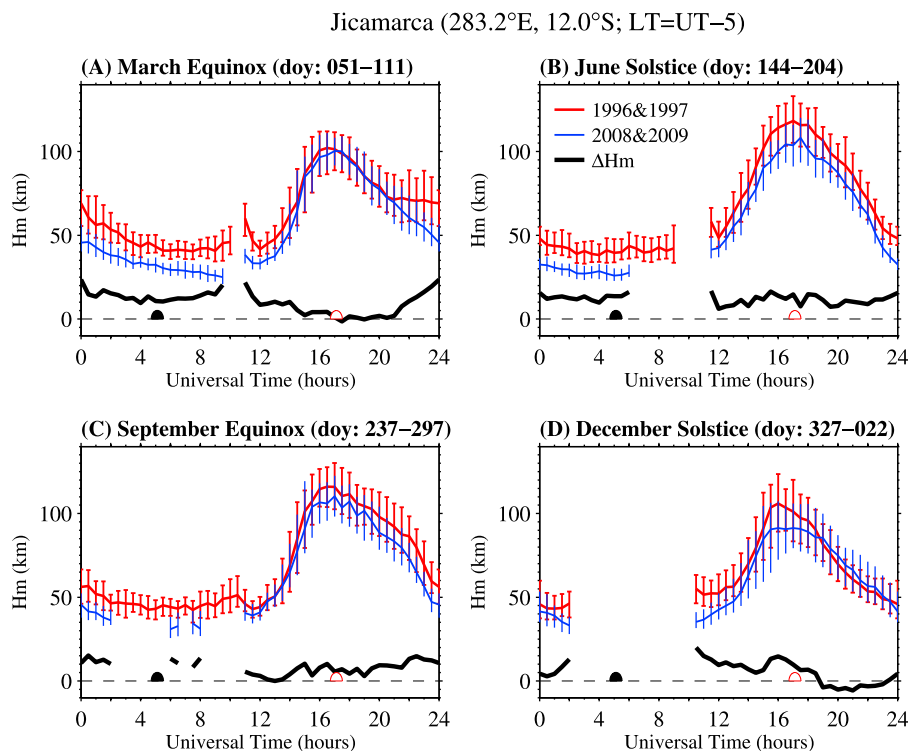


**Figure 4.** Universal time variation of  $H_m$  ( $F_2$  layer Chapman scale height) over Jicamarca in four seasons for the last two solar minima. The red and blue lines indicate the seasonal median in 1996–1997 and in 2008–2009, respectively, and black lines show  $\Delta H_m$ , the differences of seasonal median  $H_m$  between 1996 and 1997 and 2008–2009. Bars show the upper and lower quartiles. The seasonal median and upper/lower quartiles are not calculated when the number of data is below 50 points (dotted line). The local midnight and noon at Jicamarca is also indicated by the solid and open semicircle, respectively.

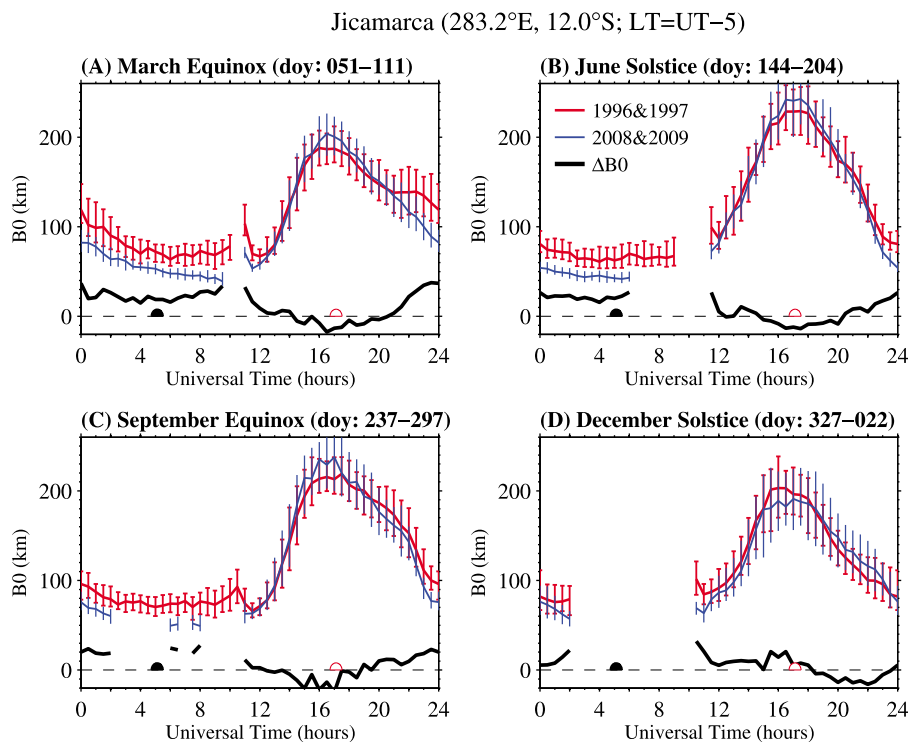


**Figure 5.** Similar to Figure 4, but for  $B_0$ , the thickness parameter of the bottomside profile. Here  $\Delta B_0$  is the difference of  $B_0$  during the last two solar minima.

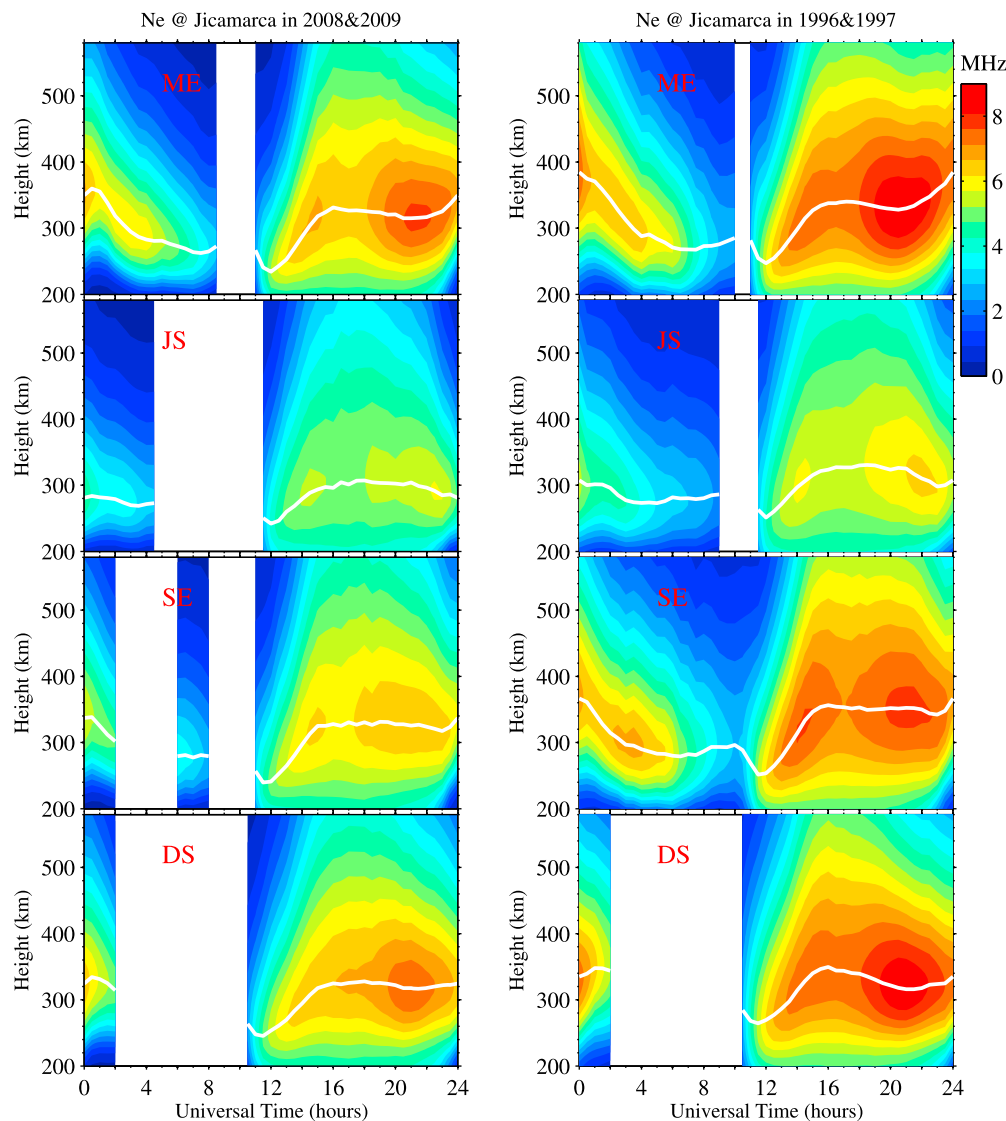


**Figure 6.** The universal time and altitude structure of seasonal average electron density (in MHz) over Jicamarca in four seasons during (left) 2008–2009 and (right) 1996–1997. The white lines indicate  $h_mF_2$ .

seasons during 2008–2009 and 1996–1997. Figure 7 plots  $\Delta N_e$ , the differences of  $N_e$  between the two groups. Positive  $\Delta N_e$  means higher  $N_e$  in 1996–1997 and negative means higher values in 2008–2009.

[25] Seeing from Figures 6 and 7, we can see that the diurnal evolution and altitudinal structure of  $N_e$  exhibit very alike pictures between the two groups, but the values of  $N_e$  in 1996–1997 overall exceed those in 2008–2009. As depicted in Figure 7, significant decrease in  $N_e$  from 1996 to 1997 to 2008–2009 occurred for the four seasons, not only in the daytime but also in the nighttime. More interesting, the amplitude of the decrease in  $N_e$  is much greater at altitudes above  $h_mF_2$  than at altitudes below  $h_mF_2$ . There is little decrease in  $N_e$  at altitudes below  $h_mF_2$  in June solstice. Furthermore, the most significant feature is the local time and seasonal differences in ionospheric response.  $\Delta N_e$  are largest in September equinox and weakest in June solstice. It is more perceptible in the afternoon hours.

[26] Taken together with the solar data listed in Table 1, one can infer that the ionosphere responds complicatedly to

the reduction in solar input. The values of  $\Delta EUV$  and  $\Delta N_e$  are the largest in September equinox. In contrast, although the values of  $\Delta EUV$  are the smallest in March equinox, the  $\Delta N_e$  are not the smallest.

#### 4. Dependence of Results on Time Scale of Analysis

[27] This analysis reveals a substantial reduction in  $f_oF_2$  over Jicamarca from 1996 to 1997 to 2008–2009, which is consistent with the previous survey with global ionosonde data by Liu *et al.* [2011a]. In contrast, Araujo-Pradere *et al.* [2011] found a minor and marginal response in  $f_oF_2$  over Boulder (40.0°N, 254.7°E), Point Arguello (35.6°N, 239.4°E), Hobart (42.9°S, 147.3°E) and Camden (34.0°S, 150.7°E). The  $f_oF_2$  data from the four middle latitude stations have also been included in the investigation by Liu *et al.* [2011a] (see Table 1 in their work for reference).

[28] It is puzzled why the works by Araujo-Pradere *et al.* [2011] and by Liu *et al.* [2011a] show different responses at the same stations to the decrease in solar input during this

$\Delta N_e$  @ Jicamarca between 1996&1997 and 2008&2009

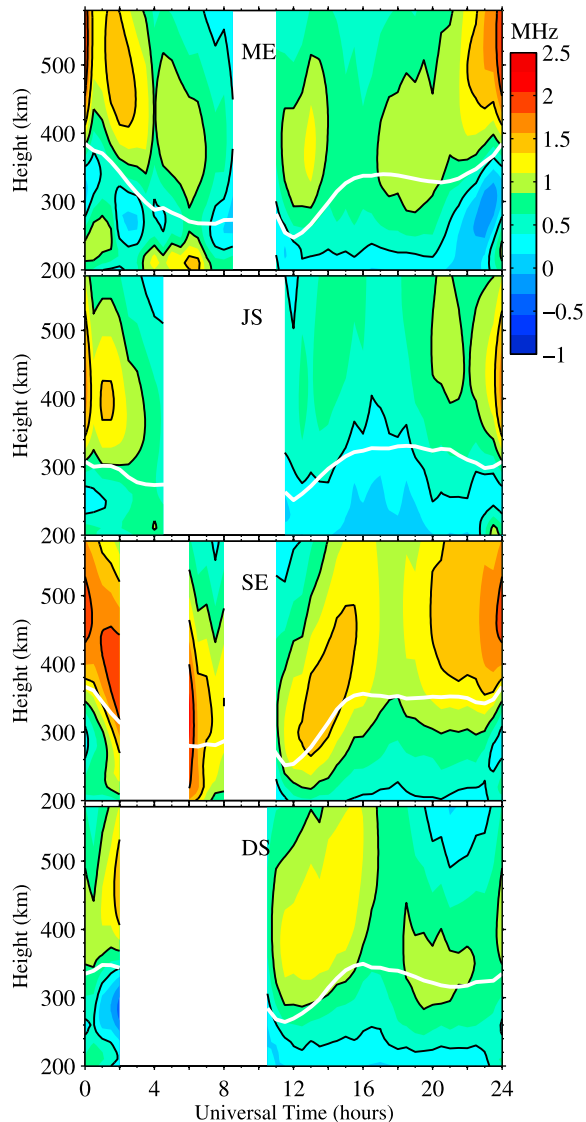


**Figure 7.** The universal time and altitude structure of  $\Delta N_e$  over Jicamarca in four seasons. Here  $\Delta N_e$  (in MHz) is the difference of electron density between 1996 and 1997 and 2008–2009. The white lines indicate  $h_m F_2$  in 1996–1997.

minimum. Admittedly, in the above investigations different approaches are adopted. Liu et al. [2011a] took a moving yearly mean, the present analysis was conducted with seasonal averaging, and Araujo-Pradere et al. [2011] used a monthly statistics. The last analysis was conducted by directly comparing with monthly average data in selected months.

[29] To look into the response in more details, in a separate study we further determined the difference of  $f_o F_2$  over Jicamarca between the two solar minima with the methods of Liu et al. [2011a] and Araujo-Pradere et al. [2011], respectively. It shows that the seasonal average and moving yearly mean values of  $f_o F_2$  in 2008–2009 fall below those in 1996–1997 all the time, and the monthly statistics exhibits little or marginal changes at some time intervals as conducted by Araujo-Pradere et al. [2011] (figures not shown).

[30] Moreover, what could provide perspective on this difference? In our view, the sensitivity of ionospheric response to the applied methods reflects the impacts of various time scales in the variability of the ionosphere. In addition to the possible regional characteristic, the ionosphere displays variations on multiply time scales. It is well known that, among the multiply time scales variability, there are distinct long-term trends, solar cycle and seasonal modulations and day-to-day variability as well [e.g., Rishbeth and Mendillo, 2001; Laštovička et al., 2006; Liu et al., 2011c]. A large part of the F layer variability is primarily driven by the modulation of solar EUV flux, and the rest are linked to that of geomagnetic activity and meteorological sources [Rishbeth and Mendillo, 2001]. Unfortunately, we cannot yet quantitatively separate the contributions from various sources, and their complexity is still a very active topic of research.

[31] To gauge the impact of changes of various time scales, we decomposed the  $f_o F_2$  data over Jicamarca to retrieve the seasonal modulations and the components over longer time scales. The longer time scales here can be treated as yearly mean values, which in essence are similar to those by Liu et al. [2011a]. We assume the  $f_o F_2$  data in a year can be represented as a superposition of annual mean and annual, semiannual, and terannual components. The results at selected times (02:00, 15:00 and 21:00 UT) are given in Table 2.

[32] We can found from Table 2, between the two solar minima, an undoubted decrease in the longer components and uncertain differences in seasonal modulations. In particular, at some times, the terannual amplitudes are greater in 2008 and 2009 than in 1996 and 1997. The variations over longer scales sometimes are hidden by large shorter-scale variations. As a consequence, in certain instances the response from solar minimum to minimum depends on the approach used.

**Table 2.** Principal Components of  $f_o F_2$  at Selected Times in 1996, 1997, 2008, and 2009<sup>a</sup>

	02:00 UT	15:00 UT	21:00 UT
	<i>Mean</i>		
6.2321 (1996)	7.1904 (1996)	7.8716 (1996)	
<b>6.7134</b> (1997)	<b>7.8333</b> (1997)	<b>8.4900</b> (1997)	
5.4909 (2008)	6.6707 (2008)	7.3895 (2008)	
5.4396 (2009)	6.4970 (2009)	7.0545 (2009)	
	<i>Annual</i>		
0.9830 (1996)	1.0798 (1996)	1.4292 (1996)	
0.9485 (1997)	<b>1.3941</b> (1997)	<b>1.5521</b> (1997)	
<b>1.2226</b> (2008)	0.8956 (2008)	1.5410 (2008)	
1.0803 (2009)	0.6473 (2009)	0.9378 (2009)	
	<i>Semiannual</i>		
0.9117 (1996)	0.6262 (1996)	0.3504 (1996)	
<b>1.2448</b> (1997)	<b>0.9002</b> (1997)	<b>0.8305</b> (1997)	
1.1424 (2008)	0.6052 (2008)	0.5987 (2008)	
0.8851 (2009)	0.5725 (2009)	0.7926 (2009)	
	<i>Terannual</i>		
0.3599 (1996)	0.1904 (1996)	0.2078 (1996)	
0.1689 (1997)	0.1761 (1997)	0.3530 (1997)	
<b>0.4671</b> (2008)	<b>0.2057</b> (2008)	0.3250 (2008)	
0.4074 (2009)	0.1759 (2009)	<b>0.4095</b> (2009)	

<sup>a</sup>Here the bold numbers show the maximum values of the amplitudes of principal components in 4 years.

[33] In short, different approaches used in the related investigations essentially are not focused on the same time scales of the changes. The reported inconsistent patterns can be understood by the inconsistent impacts of various time scale changes. It also implies the contributions from other sources, besides the effect of solar EUV flux as discussed by *Liu et al.* [2011a].

[34] In addition, it needs to be pointed out that some related investigations are made with the data of limited temporal coverage. In *Liu et al.* [2011a] the JPL-TEC data covers the years 1998–2010, but lack the data in the last solar minimum. *Lühr and Xiong* [2010] compared the satellite data for the years 2000–2009 with empirical model predictions, *Heelis et al.* [2009] used the topside data for June–August 2008, and *Liu et al.* [2011b] explored the features of the ionosphere at middle and low latitudes using 5 years of  $N_e$  profiles retrieved from radio occultation measurements of the Constellation Observing System for Meteorology, Ionosphere and Climate (COSMIC) mission. Those studies lacked the data during the last minimum for a reference. Therefore, they answered a question that whether the ionospheric behavior deviates from the expected effects of solar EUV flux.

## 5. Further Remarks

[35] According to *Rishbeth* [2004],  $h_mF_2$  is closely related to constant pressure-levels or neutral temperature in the thermosphere. The altitude a constant pressure-level rides on increases with neutral temperature. At the same time, the topside temperature structure also makes contributions to changes in  $H_m$  [*Kutiev et al.*, 2009]. There are positive correlations between  $H_m$  and  $h_mF_2$  as revealed by *Liu et al.* [2006] and *Lee and Reinisch* [2007], because neutral and ionic temperatures are positive correlated. As described in section 3, the  $F_2$  layer peak height and  $H_m$  fall lower in 2008–2009 in most instances. The upper atmosphere and ion temperature became cooler during the deep minimum [*Emmert et al.*, 2010; *Heelis et al.*, 2009; *Solomon et al.*, 2010], one therefore expects a lower  $h_mF_2$  and  $H_m$ . Thus, the expected effect of temperature cooling can consistently explain the observed nature of equatorial  $h_mF_2$  and  $H_m$ .

[36] There still remains a question regarding the link between changes in equatorial  $\mathbf{E} \times \mathbf{B}$  drift and the  $F$  layer plasma distributions. What we are interested here is the role of  $\mathbf{E} \times \mathbf{B}$  drift in the reduction in  $f_oF_2$ ,  $h_mF_2$ , and electron density profiles during the deep minimum.

[37] It is well known that the plasma  $\mathbf{E} \times \mathbf{B}$  vertical drift plays important roles in the plasma distribution and dynamics in low latitude and equatorial regions [e.g., *Fejer*, 2011]. The  $\mathbf{E} \times \mathbf{B}$  vertical drift drives the ionospheric plasma transporting across the geomagnetic field lines to higher or lower altitudes, controlling the diurnal and seasonal variations of equatorial  $f_oF_2$  and  $h_mF_2$ . There are not enough observations available for us to quantitatively determine the changes of equatorial  $\mathbf{E} \times \mathbf{B}$  vertical drift during the periods, although extensive studies using measurements, including those from the Jicamarca incoherent scatter radar, show there are solar cycle variations in equatorial  $\mathbf{E} \times \mathbf{B}$  vertical drift.

[38] However, changes in  $\mathbf{E} \times \mathbf{B}$  vertical drift during the periods can be indirectly inferred from the observation. As illustrated in Figure 7, there are discernible local time and

seasonal dependences in the differences of electron density profiles between the two minima; that is, stronger differences in electron density at Jicamarca are presented in the afternoon hours and in equinoxes. Both features are consistent with the morphology of  $\mathbf{E} \times \mathbf{B}$  vertical drift, which has been extensively studied [*Fejer*, 2011]. According to Figure 1 in the review by *Fejer* [2011],  $\mathbf{E} \times \mathbf{B}$  vertical drift over Jicamarca shows stronger solar flux dependence in the afternoon hours and in equinoxes. Thus, one could infer that the equatorial  $\mathbf{E} \times \mathbf{B}$  vertical drift has played important roles in the changes in ionospheric plasma density from solar minimum to minimum. In other words, the equatorial  $\mathbf{E} \times \mathbf{B}$  vertical drift should be smaller in 2008–2009 deep solar minimum.

[39] Furthermore, there is an inconsistency between changes in B0 and those in  $H_m$  and  $h_mF_2$ , and the electron density profiles also do not respond identically at different altitudes, strongest at altitudes above  $h_mF_2$ . It not only shows perplexed behaviors of electron density profiles over Jicamarca, but also reflects that many processes are competitively involved [*Liu et al.*, 2009]. *Smithtro and Sojka* [2005] simulated the response of the ionosphere and thermosphere to extreme solar cycle conditions. The model results recognized that the responses are different for different ions ( $O^+$  and molecular ions) and at different altitudes.

[40] Regarding the characteristics of bottomside profiles, our results agree with the work by *Lee* [2011]. *Lee* [2011] reported an equatorial B0 anomaly detected in the ionogram data from 2003 to 2008. In September, the maximum daytime B0 over Jicamarca decreased in 2003–2007 with decreasing solar activity, but this decline feature is not found in 2008. The maximum value of B0 in September 2008 is 242 km, higher than 218 km in 2007 and 218 km in 1996. They attributed this anomaly to the smaller solar sensitivity of plasma density at lower altitudes.

## 6. Summary

[41] In this investigation, we collected the 4 year ionogram data recorded at Jicamarca during the last two solar minima to comparatively study the changes in the equatorial ionosphere caused by the deep solar minimum in 2008–2009. The analysis of the ionogram-derived  $F_2$  layer parameters ( $f_oF_2$ ,  $h_mF_2$ ,  $H_m$ , and B0) and  $N_e$  profiles illustrates discernible changes in equatorial ionosphere for the deep solar minimum. The major conclusions are summarized as follows:

[42] 1. The median values of  $f_oF_2$  in the four seasons are smaller in 2008–2009 than in 1996–1997, both in the daytime and nighttime. The picture of ionospheric changes from solar minimum to minimum is related with the data analysis method used. The inconsistent changes in the published investigations reflect the impact of  $f_oF_2$  variability on the solar minimum-to-minimum difference over different time scales. The reduction in  $f_oF_2$  during the current solar cycle minimum is certainly presented in the longer time scale variations of  $f_oF_2$ .

[43] 2. During the deep solar minimum,  $h_mF_2$ ,  $H_m$ , and B0 are notably decreased at most time intervals, but their behaviors are not identical all the time. An unusual feature that higher B0 in 2008–2009 than in 1996–1997 is found at some daytime intervals.

[44] 3. The responses of electron density to the deep solar minimum are different at different altitudes, and the change in  $F$  layer profiles shows local time and seasonal differences. The change is larger in March and September equinoxes than in June and December solstices, and stronger decrease in  $N_e$  is more perceptible in the afternoon hours and at altitudes above  $h_m F_2$ .

[45] The overall picture suggests that competing processes are involved in the equatorial region. The reduction in  $f_o F_2$  and electron density is consistent with the lowest levels seen in solar extreme ultraviolet (EUV) radiance during the recent deep solar minimum. The accompanying temperature cooling can consistently explain the observed nature of equatorial  $h_m F_2$  and  $H_m E \times B$  vertical drift played a critical role in the local time and seasonal feature of changes in electron density profiles. Moreover, the inconsistent changes in  $N_e$  profiles reflect different solar sensitivity of plasma density at different altitudes to the decrease in solar EUV flux.

[46] **Acknowledgments.** The authors would like to thank B. W. Reinisch of the Center for Atmospheric Research, University of Massachusetts Lowell for the ionogram data of DIDBase. The SEM/SOHO EUV data is downloaded from the Web site: [http://www.usc.edu/dept/space\\_science/](http://www.usc.edu/dept/space_science/). The CELIAS/SEM experiment on the Solar Heliospheric Observatory (SOHO) spacecraft (SOHO is a joint European Space Agency and U.S. NASA mission). The  $F_{10.7}$  index is downloaded from the SPIDR website (available at <http://spidr.ngdc.noaa.gov/>). This research was supported by National Natural Science Foundation of China (41074112, 41174137, 40725014), National Key Basic Research Program of China (2012CB825604), and the Specialized Research Fund for State Key Laboratories.

[47] Robert Lysak thanks the reviewers for their assistance in evaluating this paper.

## References

- Araujo-Pradere, E. A., R. Redmon, M. Fedrizzi, R. Viereck, and T. J. Fuller-Rowell (2011), Some characteristics of the ionospheric behavior during the solar cycle 23–24 minimum, *Sol. Phys.*, doi:10.1007/s11207-011-9728-3, in press.
- Bilitza, D., S. M. Radicella, B. W. Reinisch, J. O. Adeniyi, M. E. Gonzalez, S. R. Zhang, and O. Obrou (2000), New B0 and B1 models for IRI, *Adv. Space Res.*, 25, 89–95, doi:10.1016/S0273-1177(99)00902-3.
- Chen, Y., L. Liu, and W. Wan (2011), Does the  $F_{10.7}$  index correctly describe solar EUV flux during the deep solar minimum of 2007–2009?, *J. Geophys. Res.*, 116, A04304, doi:10.1029/2010JA016301.
- Didkovsky, L. V., D. L. Judge, and S. R. Wieman (2010), Minima of solar cycles 22/23 and 23/24 as seen in SOHO/CELIAS/SEM absolute solar EUV flux, in *SOHO-23: Understanding a Peculiar Solar Minimum*, edited by S. R. Cranmer, J. T. Hoeksema, and J. Kohl, *ASP Conf. Ser.*, 428, 73–80.
- Emmert, J. T., J. L. Lean, and J. M. Picone (2010), Record-low thermospheric density during the 2008 solar minimum, *Geophys. Res. Lett.*, 37, L12102, doi:10.1029/2010GL043671.
- Fejer, B. G. (2011), Low latitude ionospheric electrodynamics, *Space Sci. Rev.*, 158, 145–166, doi:10.1007/s11214-010-9690-7.
- Gibson, S. E., J. U. Kozyra, G. de Toma, B. A. Emery, T. Onsager, and B. J. Thompson (2009), If the Sun is so quiet, why is the Earth ringing? A comparison of two solar minimum intervals, *J. Geophys. Res.*, 114, A09105, doi:10.1029/2009JA014342.
- Gulyaeva, T. L. (1987), Progress in ionospheric informatics based on electron-density profile analysis of ionograms, *Adv. Space Res.*, 7, 39–48, doi:10.1016/0273-1177(87)90269-9.
- Heelis, R. A., W. R. Coley, A. G. Burrell, M. R. Hairston, G. D. Earle, M. D. Perdue, R. A. Power, L. L. Harmon, B. J. Holt, and C. R. Lippincott (2009), Behavior of the O<sup>+</sup>/H<sup>+</sup> transition height during the extreme solar minimum of 2008, *Geophys. Res. Lett.*, 36, L00C03, doi:10.1029/2009GL038652.
- Huang, X., and B. W. Reinisch (1996), Vertical electron density profile from the Digisonde network, *Adv. Space Res.*, 18, 121–129, doi:10.1016/0273-1177(95)00912-4.
- Huang, X., and B. W. Reinisch (2001), Vertical electron content from ionograms in real time, *Radio Sci.*, 36, 335–342, doi:10.1029/1999RS002409.
- Judge, D., et al. (1998), First solar EUV irradiances obtained from SOHO by the Cielias/SEM, *Sol. Phys.*, 177, 161–173, doi:10.1023/A:1004929011427.
- Kutiev, I., P. Marinov, A. Belehaki, B. Reinisch, and N. Jakowski (2009), Reconstruction of topside density profile by using the topside sounder model profiler and Digisonde data, *Adv. Space Res.*, 43, 1683–1687, doi:10.1016/j.asr.2008.08.017.
- Laštovička, J., et al. (2006), Long-term trends in foF2: A comparison of various methods, *J. Atmos. Sol. Terr. Phys.*, 68, 1854–1870, doi:10.1016/j.jastp.2006.02.009.
- Lee, C.-C. (2011), Equatorial B0 anomaly in September under extremely low solar activity, *J. Geophys. Res.*, 116, A05325, doi:10.1029/2010JA016394.
- Lee, C.-C., and B. W. Reinisch (2007), Quiet-condition variations in the scale height at F2-layer peak at Jicamarca during solar minimum and maximum, *Ann. Geophys.*, 25, 2541–2550, doi:10.5194/angeo-25-2541-2007.
- Lee, C.-C., B. W. Reinisch, S. Y. Su, and W. S. Chen (2008), Quiet-time variations of F2-layer parameters at Jicamarca and comparison with IRI-2001 during solar minimum, *J. Atmos. Sol. Terr. Phys.*, 70, 184–192, doi:10.1016/j.jastp.2007.10.008.
- Liu, L., W. Wan, and B. Ning (2006), A study of the ionogram derived effective scale height around the ionospheric hmF2, *Ann. Geophys.*, 24, 851–860, doi:10.5194/angeo-24-851-2006.
- Liu, L., H. Le, W. Wan, M. P. Sulzer, J. Lei, and M.-L. Zhang (2007), An analysis of the scale heights in the lower topside ionosphere based on the Arecibo incoherent scatter radar measurements, *J. Geophys. Res.*, 112, A06307, doi:10.1029/2007JA012250.
- Liu, L., W. Wan, B. Ning, and M.-L. Zhang (2009), Climatology of the mean TEC derived from GPS global ionospheric maps, *J. Geophys. Res.*, 114, A06308, doi:10.1029/2009JA014244.
- Liu, L., Y. Chen, H. Le, V. I. Kurkin, N. M. Polekh, and C. C. Lee (2011a), The ionosphere under extremely prolonged low solar activity, *J. Geophys. Res.*, 116, A04320, doi:10.1029/2010JA016296.
- Liu, L., H. Le, Y. Chen, M. He, W. Wan, and X. Yue (2011b), Features of the middle and low latitude ionosphere during solar minimum as revealed from COSMIC radio occultation measurements, *J. Geophys. Res.*, 116, A09307, doi:10.1029/2011JA016691.
- Liu, L., W. Wan, Y. Chen, and H. Le (2011c), Solar activity effects of the ionosphere: A brief review, *Chin. Sci. Bull.*, 56, 1202–1211, doi:10.1007/s11434-010-4226-9.
- Lühr, H., and C. Xiong (2010), The IRI-2007 model overestimates electron density during the 23/24 solar minimum, *Geophys. Res. Lett.*, 37, L23101, doi:10.1029/2010GL045430.
- Raju, P. T. S., and M. M. Rao (1975), Influence of magnetic declination on the noon bite-out phenomenon of the equatorial F2 region, *Indian J. Radio Space Phys.*, 4, 44–45.
- Reinisch, B. W., I. A. Galkin, G. Khmyrov, A. Kozlov, and D. F. Kitrosser (2004a), Automated collection and dissemination of ionospheric data from the Digisonde network, *Adv. Radio Sci.*, 2, 241–247, doi:10.5194/ars-2-241-2004.
- Reinisch, B. W., X. Huang, A. Belehaki, J. Shi, M. Zhang, and R. Ilma (2004b), Modeling the IRI topside profile using scale height from ground-based ionosonde measurements, *Adv. Space Res.*, 34, 2026–2031, doi:10.1016/j.asr.2004.06.012.
- Rishbeth, H. (2004), Questions of the equatorial F2-layer and thermosphere, *J. Atmos. Sol. Terr. Phys.*, 66, 1669–1674, doi:10.1016/j.jastp.2004.07.008.
- Rishbeth, H., and M. Mendillo (2001), Patterns of F2-layer variability, *J. Atmos. Sol. Terr. Phys.*, 63, 1661–1680, doi:10.1016/S1364-6826(01)00036-0.
- Russell, C. T., J. G. Luhmann, and L. K. Jian (2010), How unprecedented a solar minimum?, *Rev. Geophys.*, 48, RG2004, doi:10.1029/2009RG000316.
- Smithro, C. G., and J. J. Sojka (2005), Behavior of the ionosphere and thermosphere subject to extreme solar cycle conditions, *J. Geophys. Res.*, 110, A08306, doi:10.1029/2004JA010782.
- Solomon, S. C., T. N. Woods, L. V. Didkovsky, J. T. Emmert, and L. Qian (2010), Anomalous low solar extreme-ultraviolet irradiance and thermospheric density during solar minimum, *Geophys. Res. Lett.*, 37, L16103, doi:10.1029/2010GL044468.
- Solomon, S. C., L. Qian, L. V. Didkovsky, R. A. Viereck, and T. N. Woods (2011), Causes of low thermospheric density during the 2007–2009 solar minimum, *J. Geophys. Res.*, 116, A00H07, doi:10.1029/2011JA016508.
- Tulasi Ram, S., S.-Y. Su, C. H. Liu, B. W. Reinisch, and L.-A. McKinnell (2009), Topside ionospheric effective scale heights (HT) derived with ROCSAT-1 and ground-based ionosonde observations at equatorial and midlatitude stations, *J. Geophys. Res.*, 114, A10309, doi:10.1029/2009JA014485.

Y. Chen, H. Le, L. Liu, W. Wan, and J. Yang, Beijing National Observatory of Space Environment, Institute of Geology and Geophysics, Chinese Academy of Sciences, Beijing 100029, China. (liul@mail.iggcas.ac.cn)  
C.-C. Lee, General Education Center, Ching-Yun University, Zhongli 320, Taiwan.